RSC Advances

This is an *Accepted Manuscript*, which has been through the Royal Society of Chemistry peer review process and has been accepted for publication.

Accepted Manuscripts are published online shortly after acceptance, before technical editing, formatting and proof reading. Using this free service, authors can make their results available to the community, in citable form, before we publish the edited article. This *Accepted Manuscript* will be replaced by the edited, formatted and paginated article as soon as this is available.

You can find more information about *Accepted Manuscripts* in the Information for Authors.

Please note that technical editing may introduce minor changes to the text and/or graphics, which may alter content. The journal's standard Terms & Conditions and the Ethical guidelines still apply. In no event shall the Royal Society of Chemistry be held responsible for any errors or omissions in this *Accepted Manuscript* or any consequences arising from the use of any information it contains.

ROYAL SOCIETY OF CHEMISTRY

www.rsc.org/advances

Fabrication of silver nano powder embedded kraton polymer actuator and its characterization

Ajahar Khan[a], Inamuddin[a,*], R.K. Jain[b], Mu. Naushad[c]

[a] Department of Applied Chemistry, Faculty of Engineering and Technology, Aligarh Muslim University (AMU), Aligarh, 202002, India

[b] CSIR-Central Mechanical Engineering Research Institute, (CSIR-CMERI), Durgapur, 713209, West Bengal, India

[c] Department of Chemistry, College of Science, Building # 5, King Saud University, Riyadh, Saudi Arabia

Abstract

A novel silver nano powder (Ag Pw) embedded kraton (KR) ionic polymer actuator was fabricated**.** The KR-Ag-Pw ionic polymer metal composite (IPMC) membrane was prepared by a solution casting method. IPMC membrane shows good electro-mechanical, ion exchange and water retention (WR) and proton conductivity (PC) properties which are responsible for the high performance of ionic polymer actuator. The physicochemical properties of the KR-Ag-Pw ionic polymer actuator were determined using X-ray diffraction, Fourier transform infra-red spectroscopy (FTIR), scanning electron microscopy (SEM) and thermogravimetric analysis (TGA) studies. After applying a voltage (0-3.5 V DC), the maximum bending behaviour is achieved upto 17 mm. By constructing a multi KR-Ag-Pw IPMC fingers based gripper, it is proved that this kind of actuator has potential in robotic application.

Keywords: KR-Ag-Pw IPMC, Water uptake, ion exchange capacity, proton conductivity, FT-IR, TGA, SEM, XRD, electrical property, water loss, bending behaviour.

RSC Advances Accepted Manuscript

1. Introduction

The polymeric actuators produce mechanical responses by various external stimuli [1–3]. Principally, actuators are able to transduce an input electrical energy to an output mechanical energy [4-7]. This property can be very well utilized to develop artificial muscle [8,9], active catheters [10,11] and biomimetic robots [12-15]. A variety of electrical energy responsive polymers such as ionic polymer metal composites (IPMCs) [16,17], ionic polymer gels [18], conductive polymers [19,20] piezoelectric polymers and dielectric elastomers [21,22] have been widely used in making artificial muscles and microrobots. Among the different types of polymeric actuators the IPMC actuators consisting of ionic polymer material sandwiched between two platinum electrode layers have been widely used for the fabrication of applied actuators [23]. The IPMC actuators have several outstanding properties including light weight, low applied voltage, good bending actuation, flexibility, easy molding into different shapes and so on [24-27]. However, a time-consuming electroless plating process for deposition of Pt or Au electrode layers on both side of polymer membrane is usually necessary in the fabrication of IPMCs membrane actuator. Since an external electrical potential is required to induce the actuator motion. Therefore, metal electroplating [24] or combination of electroless and electroplating techniques [28] requiring a relatively long processing time for the fabrication of Pt or Au electrode layers on the surfaces of the ionic polymer composite membrane. To alternate this time consuming and expensive method for the preparation of IPMCs membrane, a simpler and more cost effective fabrication technique is developed. In this method kraton, a sulphonated polymer and silver nano powder were mixed together and used to fabricate the ionic polymer actuator by solution casting method. Sulfonated polymers are generally used as ionic polymer metal composite actuator [29–33] due to their good electromechanical and chemical properties, water uptake and high proton conductivity. Kraton is a sulfonated ionomeric polymer that posses outstanding

RSC Advances Accepted Manuscript

electromechanical thermal and chemical stabilities and good film-forming capability [34]. The silver nano particles show excellent electrical, thermal, and mechanical properties like other Pt or Au metal electrodes. The KR-Ag-Pw IPMC provides an easy and reliable realization of versatile novel ionic polymer actuators as well as possibility of industrial applications.

RSC Advances Accepted Manuscript

2. Experimental

2.1. Materials

A non-perfluorinated kraton [pentablock copolymer poly((t-butyl-styrene)-b-(ethylene-r-propylene)-b-(styrene-r-styrene sufonate)-b-(ethylene-r-propylene)-b-(t-butyl-styrene) (tBS-EP-SS-EP-tBS))](Nexar MD9200) (Nexar Polymer, USA), silver nanopowder with a particle size range of 20-40 nm and tetrahydrofuran (THF) (Thermo Fisher Scientific Pvt. Ltd., India), were used as received. Characteristic properties of Kraton MD9200 polymer based on Kraton Polymers Group of Companies data document catalogue number K00491 dated October 2008 is given in Supplementary information Table 1.

2.2 Fabrication of membrane

The fabrication of membrane was started by dissolving 3 g of kraton (KR) polymer in 20 ml THF at room temperature (25±3 °C) with constant stirring upto 8 h. After complete dissolution 0.3 g silver nano powder (Ag-Pw) was added with constant stirring for 4 h at room temperature (25±3 °C). The obtained solution was cast in a petri dish (50 × 17 mm) and covered with Whatman filter paper (No. 1) for slow evaporation of the THF at room temperature (25±3 °C). After complete evaporation of THF the KR-Ag-Pw composite polymer membrane was taken out from petri dish. Now, the fabricated membrane was ready for further studies.

2.3. Water retention capacity

The water retention capability of KR-Ag-Pw IPMC membrane was determined by a water retention (WR) experiments as reported elsewhere [34]. The water retention of the KR-Ag-PW membranes were calculated by immersing the preweighed membranes into the distilled

RSC Advances Accepted Manuscript

water at room temperature (25 ºC±3), 45 ºC and 65 ºC for different times 2-24 h. The WR capacity was calculated by applying the following equation:

$$W = \frac{W_{wet} - W_{dry}}{W_{dry}} \times 100 \quad \text{…….....1}$$

where W_{wet} and W_{dry} are the weights of the wet and the dried membranes, respectively.

2.4. Ion exchange capacity (IEC)

The IEC of the membrane was calculated using a conventional titration method. First, the KR-Ag-Pw ionic polymer membrane was immersed in 1 M HNO_3 for 24 h to convert into H^+ form. The ionic polymer membrane was washed with distilled water till neutral and dried. The dried membrane was cut into small pieces and packed into glass column. Now, 1 M $NaNO_3$ was passed through the column with a very slow flow rate (0.5 ml $minute^{-1}$) to convert the membrane into Na^+ form. The dissociated H^+ ions were then titrated with 0.1 M NaOH solution using phenolphthalein as indicator. The IEC value of IPMC membrane was calculated by using equation 2.

$$\text{Ion exchange capacity} = \frac{Volume\,of\ NaOH\ consumed \times Normality\,of\ NaOH}{Weight\,of\ the\,dry\,membrane}\,(meq\,g^{-1}\ of\ membrane)$$

……..2

2.5. Water loss

To determine the water loss KR-Ag-Pw ionic polymer membrane was first immersed in DMW for 12 h at 45 ºC and weighed, the water loss of the ionic polymer membrane was calculated by weighing the KR-AgPw membrane after applying an electric potential of 3-6 V for different interval of time 3-9 min. The water loss of the membrane actuator was calculated by following equation 3.

RSC Advances Accepted Manuscript

$$\% \text{ Water loss} = \frac{W_1 - W_2}{W_1} \times 100 \quad \text{.....3}$$

Where, W_1 and W_2 are the weight of wet membrane and weight of membrane after applied electric potential, respectively.

2.6. Proton conductivity (PC)

PC (σ) of the fully hydrated ionic polymer membrane (1×3 cm^2) was determined at room temperature by an impedance analyzer (FRA32M.X), connected with Autolab 302N modular potentiostate/galvanostate; over a frequency of 100 KHz and an AC perturbation of 10 mV. The PC of membrane was calculated by the following equation 4:

$$\sigma = \frac{L}{R \times A} \text{ ……..4}$$

where σ is proton conductivity in (S cm^{-1}), L is the thickness of membrane in (cm), A is cross-sectional area of membrane (cm) and R is the resistance (ohm).

2.7. Characterization of KR-Ag-Pw membrane actuator

Structural features of KR-AgPw polymer membranes were characterized by Fourier transform infrared spectroscopy (FTIR) (Perkin Elmer Spectrometer, USA) and X-ray diffraction (XRD) (Rigaku, miniflex-II, Japan) with Cu Kα. Scanning electron microscopic images were captured to observe the surface morphology and cross-sectional view of KR-Ag-Pw ionomeric polymer membrane with the help of scanning electron microscope (SEM Jeol, JSM-6510LV, Japan). Thermal stability of KR-Ag-Pw composite polymer membrane was determined by thermal gravimetric analysis (TGA) (TGA analyser (TGA pyres 1-HT, Perkin Elmer, USA) at a heating rate of 10 °C min^{-1} in N_2 atmosphere. The cyclic voltammetry (CV)

RSC Advances Accepted Manuscript

and linear sweep voltammetry (LSV) (Autolab 302N modular potentiostate/galvanostate) were carried out in DMW at triangle voltage input of 3.5 V with a step potential of 50 mV s^{-1}.

2.8. Electromechanical characterization

In order to obtain the bending behavior of KR-Ag-Pw based IPMCmembrane actuator, an electromechanical characterization is required. For analyzing this bending behavior with voltage, the schematic diagram of experimental setup is shown in **Fig. 1** where the nano silver powder coated ionic polymer membrane IPMC is used during the experiments. The IPMC is integrated in vertical cantilever configuration on the mounting bench. A voltage (0-3.5 V DC) is sent to ionic polymer membrane with the facility of a computer interface control system which consists of computer, digital to analog card (DAC) and micro controller. An amplifier circuit is developed for providing the current rating of 50-200 mA to KR-Ag-Pw membrane so that membrane actuator can attain the maximum bending. For providing the electrical signal, both surfaces of KR-Ag-Pw strip are connected to voltage supply which is controlled by micro controller. An input command is sent to membrane actuator through a micro controller. An optical/laser displacement sensor is mounted in front of the KR-Ag-Pw based membrane actuator for finding the displacement behavior. A converter is also integrated with this sensor for switching the data transmission protocol (RS-485 to RS-232 standard). This sensor is used as feedback device while sending the pulses to it. An appropriate program is developed to interpret data which is recorded by Docklight software and provides the exact bending behavior of IPMC according to the applied potential. The bending behavior of KR-Ag-Pw based membrane actuator is shown in **Fig. 2** and the opposite behavior can also be achieved by changing the voltage polarity.

RSC Advances Accepted Manuscript

3. Results and discussion

To investigate the performance of the fabricated KR-Ag-Pw membrane actuator employing the Ag nano-powder electrodes, fundamental properties such as WR, IEC and PC were determined. The bending behaviour of IPMCs membrane under an applied electric potential is based on migration of cations along with water molecules towards cathode. The higher water retention capacity of IPMC membrane will produce better performance of IPMC actuator [35]. **Fig. 3** showed that the water retention capacity of KR-Ag-Pw membrane increases with the increase in temperature from room temperature (25 ± 3 $^{\circ}$C) to 65 ºC upto 12 h of immersion then after slightly decreases. The maximum water retention capacity of KR-Ag-Pw membrane was found to be 192.3% at room temperature (25 ± 3 $^{\circ}$C), 222.2 % at 45 $^{\circ}$C and 233.6 % at 65 ºC for 12 h of immersion time. High water retention capacity is assigned due to presence of $-SO_3$ groups in KR-Ag-Pw membrane which is considered valuable for better performance in terms of bending actuation. The IEC and PC of KR-AgPw ionic polymer membrane was found to be 2 meq g^{-1} and 1.87×10^{-3} S cm^{-1}, respectively. The high PC of KR-AgPw ionic polymer membrane will enable the better performance due to the transfer of more protons through the membrane. The high ion exchange capacity of KR-AgPw ionic polymer membrane allows higher level of water retention and also permits that more Ag particles deeply imbed in the ionic polymer membrane. Higher the Ag metal particles in the membrane actuator lower will be the resistance, hence enables the fast and large bending performance [35-36]. The high PC of KR-Ag-Pw membrane actuator shows that more hydrated cations can move quickly toward the cathode side with a large and fast actuation [36]. One of the fundamental factors for the short life time and lower repeated response of ionic polymer actuators is the water loss from the membrane actuator. After applying electric potential water loss start from the KR-Ag-Pw ionic polymer membrane due to electrolysis, from the cracks on the surface of membrane and due to natural evaporation. It

RSC Advances Accepted Manuscript

is clear from the Fig. 4 that water loss from the KR-Ag-Pw IPMC membrane actuator increases with the increase in applied voltage from 3-6 V for the same period of time. **Fig. 4** shows the maximum water loss of 40% at 6 V for 9 min. Hence, this low water loss indicates the better performance of KR-Ag-Pw ionic polymer membrane actuator [37].

To confirm the cause of failure, the scanning electron microscopic micrographs before and after actuation experiment were observed to evaluate the changes in the surface morphology. The smooth surface of kraton ionic polymer membrane without adding silver metal particles are clearly shown in the **Fig. 5 a**. The surface morphology of kraton ionic polymer with silver metal particles (KR-Ag-Pw) before and after actuation is shown in **Fig. 5** (b and d) and **Fig. 5** (c and e), respectively. SEM micrographs (**Fig. 5** (f) and (g)) at higher magnification clearly show the deposition of silver metal particles on the surface of membrane actuator. As clearly shown in the **Fig. 5** (c and e) no surface crack and cavity was observed after applying electrical potential. Hence, due to no significant change in the surface morphology of KR-Ag-Pw ionic polymer actuator membrane after applied electrical potential main cause of water loss from the membrane is considered due to electrolysis and natural evaporation.

The FTIR spectra of the KR and KR-Ag-Pw ionic polymer membrane are shown in **Fig. 6.** The bands at ~3600 cm^{-1} are assigned to sulfonic acid groups O–H vibration, other bands at around ~1080 and ~1036 cm^{-1} are due to presence of S=O stretching vibration which are confirming the existence of block styrene sulfonate unit of kraton polymer [38]. The sharp bands around 1600 and 1450 cm^{-1} can be ascribed due to the C=C stretching vibration of kraton pentablock copolymer. The spectrum shows strong absorbance peaks around 2980 to 2860 and 920 cm^{-1} which may be ascribed due to the C-H asymmetric stretching of the polymer component [39]. From the FTIR analysis it is observed that after adding silver nano powder into the KR polymer the intensity of the peaks reduces.

RSC Advances Accepted Manuscript

The TGA curve of the ionic membrane actuator is shown in **Fig. 7**. The thermal decomposition pattern of actuator membrane shows thermal stability hence function of ionic polymer actuator. The KR and KR-Ag-Pw membrane actuators display thermal stability up to 350 ºC. The TGA curve (**Fig. 7**) of the membrane actuators showed weight loss of mass (about 14 and 22 %) upto 200 ºC, which is attributed to the presence of moisture. The transition (60 and 34% weight loss) around 400 ºC may be due to the thermal degradation of sulphonic acid groups. At 400 ºC onwards, a smooth horizontal section which represents the complete formation of the oxide form of the membranes. It is clear from the TGA analysis that after adding silver nano powder into the KR polymer thermal stability of KR-Ag-Pw polymer membrane actuator is increased.

Fig. 8 clearly showed the XRD spectra of KR polymer membrane and KR-Ag-Pw polymer membrane actuator. The X-ray diffraction pattern of KR polymer membrane having very small peaks of 2θ values (**Fig. 8**), which indicates an amorphous nature of KR polymer membrane. X-ray diffraction pattern of this KR-Ag-Pw ionomeric polymer membrane shows sharp peaks of 2θ values. The analysis of these signal peaks supports towards its crystalline nature (Fig. 6). The XRD analysis reveals that KR polymer is amorphous in nature and after addition of silver nano powder it is crystalline in nature.

The electrochemical performance of the KR-Ag-Pw ionic polymer actuator was analyzed using cyclic voltammetry (CV) for this a current-voltage (I-V) hysteresis curve was recorded under 3.5 V triangle voltage input with a scan rate of 50 mV s^{-1}. Under harmonic excitation, the area under graph as shown in **Fig. 9** corresponds to the dissipated electrical energy of the actuator. It is clear from the **Fig. 10** that as the applied electric potential increases from 1 to 3.5 V while current density of KR-Ag-Pw membrane is also constantly increases. It means that the tip displacements of the KR-Ag-Pw have a proportional relationship with the dissipated power according to the increase of the driving voltages.

RSC Advances Accepted Manuscript

After applying a voltage (0-3.5 VDC), the figures of the bending characteristic of KR-Ag-Pw based membrane actuator is shown in **Fig. 11**. The experimental data of deflection are taken as given in **Table 1**. During experiments, the small size of KR-Ag-Pw membrane actuator like 30 mm length, 10 mm width, 0.08 mm thickness is taken which is cut from large fabricated sheet.

After acquiring the data, the bending characteristic with voltage is plotted as shown in **Fig. 12**. From this figure it is envisaged that when voltage is reduced, the ionic polymer membrane deflection does not reach at the same value. The deflection error is found to be 1.5 mm. This is controlled through PD controller where we can adjust the frequency for minimizing this and achieve the similar path at desired voltage. When we are applying the voltage to actuator, the actuation speed varies linearly and provides the steady state behaviour.

In order to measure the force characteristic of KR-Ag-Pw based ionic actuator membrane actuator is clamped in a cantilever configuration a fixture. The outline of testing setup is shown in Supplementary information Figure 1 **(a).** The tip of membrane actuator touches with pan of load cell when we are applying the voltage to membrane actuator as shown in Supplementary information **Figure 1 (b)**. The low force measurement load cell/weighing scale is used to find the load. The Model of Citizon (Model No. CX-220, Make: India) is used which can compute the load ranging from 0.0001- 220g. The tip of membrane actuator bends upward and downward while actuator is in operation. The movement of membrane actuator depends upon polarity of voltage. Initially, membrane actuator is kept in a horizontal cantilever configuration at certain distance because during operation the tip of membrane actuator will be touched the pan of load cell properly. The different load values are taken through load cell at voltage by conducting experiments. These force values are denoted as F_1, F_2, F_3, F_4 and F_5 respectively as given in **Table 2**. The maximum force the actuator at

RSC Advances Accepted Manuscript

different voltages is plotted as shown in **Fig. 13** which shows the maximum force value at 3.5 V is 4.60 mN.

After collecting the data of different force values with voltage range (0-3.5V), the standard deviation (SD) is calculated. Subsequently, the mean value of force is calculated by taking the average of force as given in **Table 2**. At this mean force value, the standard deviation (SD) is found and the normal/bell distribution function for KR-Ag-Pw actuator is plotted as **Fig. 14**. The actuation strain percentage is also critical property for evaluation of performance of the actuator. The strain with time of this actuator is evaluated as shown in **Fig. 15.** The maximum strain of this actuator shows the state behavior with 9326 micro strain. The comparison of this actuator (KR-Ag-Pw IPMC) and other IPMC actuators is given in Table 3. In order to prove the application of this actuator, novel KR-Ag-Pw ionic actuators based compliant multi gripping system is fabricated as shown in **Fig. 16** where the four KR-Ag-Pw ionic actuator based fingers are attached with a circular base. The actuation of the fingers is given through controlled voltage rather than using the conventional motor. By actuating these fingers, the gripping system shows the handling capability for light weight object and each finger adjusts the alignment during dexterous handling. This handling capability using KR-Ag-Pw based ionic actuator demonstrates the potential of robotic application for light weight object in industry.

4. Conclusion

In this paper, a novel kraton ionic polymer actuator with silver nano powder electrodes is fabricated by using simple solution casting methods. It is found that the fabricated ionic polymer actuator has higher water uptake, proton conductivity, and low water loss after applying the electric potential which provides the better performance as compared to kraton ionic polymer actuator. By conducting the experiments on the electrical property, the KR-Ag-

RSC Advances Accepted Manuscript

Pw ionic polymer actuator membrane was found to have enough electrical conductivity for the bending application. By performing electromechanical characterization, it is found that KR-Ag-Pw ionic polymer actuator membrane shows the maximum bending response upto 17 mm which is quite reasonable deflection for handling the object. By developing a micro gripping system, it is proved that KR-Ag-Pw actuator has the future in robotic applications.

Acknowledgement

The authors are thankful to Department of Applied Chemistry, Aligarh Muslim University, India for publishing the paper and granting the permission research facilities. Dr. Inamuddin is thankful to the Department of Science and Technology for awarding the Young Scientist award under Project no. SR/FT/CS-159/2011. The authors are also thankful to CSIR-CMERI, Durgapur, India for characterizing the electromechanical behavior of IPMC and development of IPMC based micro robotic system at DMS/Micro Robotics Laboratory, CSIR-CMERI, Durgapur, India. One of the authors (Mu. Naushad) acknowledges the King Saud University, Deanship of Scientific Research, College of Science Research Center for the support.

RSC Advances Accepted Manuscript

Reference

[1] R. H. Baughman, Synth. Met., 1996, **78**, 339–353.

[2] E. Smela, Adv. Mater., 2003, **15**, 481–494.

[3] J. D. W. Madden, N. A. Vandesteeg, P. A. Anquetil, P. G. A. Madden, A. Takshi, R. Z. Pytel, S. R. Lafontaine, P. A. Wieringa and I. W. Hunter, IEEE J. Ocean Eng., 2004, **29**, 706–728.

[4] X. Lin, J. Li, E. Smela and S. Yip, Int. J. Quantum Chem., 2005, **102**, 980–985.

[5] X. Lin, J. Li and S. Yip, Phys. Rev. Lett., 2005, **95**, 198303.

[6] M. T. Cortés and J. C. Moreno, e- Polymers, 2003, **41**, 1–42.

[7] E. Smela, MRS Bull., 2008, **33,** 197–204.

[8] Y. B. Cohen, 1st ed., SPIE Press, Washington, 2001.

[9] R. K. Jain, S. Datta, S. Majumder and A. Dutta, (2011) Int J Adv Robotic Syst, 2011 **8**, 1-9.

[10] H. H. Lin, B. K. Fang, M. S. Ju and C. C. K. Lin, J. Intell. Mater. Syst. Struct., 2009, **20**, 273–282.

[11] R. K. Jain, S. Majumder, A. Dutta, Robot Autonom Syst, 2013, **61**, 297-311.

[12] M. Shahinpoor, Electrochim. Acta, 2003, **48**, 2343–2353.

[13] S. W. Yeom and I. K. Oh, Smart Mater. Struct., 2009, **18**, 085002–085012.

[14] R. K. Jain, A. Datta and A Majumder, Mechatronics, 2013, **23**, 381-394.

RSC Advances Accepted Manuscript

[15] R. K. Jain, A. Datta and S. Majumder, Mechanics Based Design of Structures and Machines: An International Journal, 2014, 42(3):398–417.

[16] M. Shahinpoor and K.J. Kim, Smart Mater. Struct., 2001, **10**, 819–833.

[17] K. J. Kim and M. Shahinpoor, Smart Mater. Struct., 2003, **12**, 65–79.

[18] Y. Osada, H. Okuzaki and H. Hori, Nature, 1992, **355**, 242–244.

[19] E. Smela, Adv. Mater., 2003, **15,** 481–494.

[20] R. H. Baughman, C. Cui, A. A. Zakhidov, Z. Iqbal, J. N. Barisci, G. M. Spinks, G. G. Wallace, A. Mazzoldi, D. De Rossi, A. G. Rinzler, O. Jaschinski, S. Roth and M. Kertesz, Science, 1999, **284**, 1340–1344.

[21] R. Pelrine, R. Kornbluh, Q. Pei and J. Joseph, Science, 2000, **287,** 836–839.

[22] J. Kim, S. Yun and Z. Ounaies, Macromolecules, 2006, **39**, 4202–4206.

[23] M. Shahinpoor, K. J. Kim, Smart Mater. Struct., 2001, **10**, 819−833.

[24] F. Carpi and E. Smela, Wiley, West Sussex, 2009.

[25] K. J. Kim and S. Tadokoro, Springer, Berlin, 2007.

[26] E. Smela, Adv. Mater., 2003, **15,** 481-494.

[27] H. R. Choi, K. Jung, S. Ryew, J. D. Nam, J. Jeon, J. Koo and K. Tanie, IEEE-ASME Trans. Mechatron., 2005, **10**, 581-593.

[28] J. H. Jeon, S. W. Yeom and I. K. Oh, Compos. Pt. A e Appl. Sci. Manuf., 2008, **39**, 588-596.

[29] X. L. Wang, I. K. Oh, J. Lu, J. Ju and S. Lee, Mater. Lett., 2007, **61**, 5117–5120.

RSC Advances Accepted Manuscript

[30] J. H. Jeon, S. P. Kang, S. Lee and I. K. Oh, Sens. Actuators B, 2009, **143**, 357–364.

[31] X. L. Wang, I. K. Oh and T. H. Cheng, Polym. Int., 2010, **59**, 305–312.

[32] X. L. Wang, I. K. Oh and L. Xu, Sensor Actuator B Chem, 2010, **145**, 635–642.

[33] A. K. Phillips and R. B. Moore, Polymer, 2005, **46**, 7788–7802.

[34] Inamuddin, A. Khan, M. Luqman and A.Dutta, Sensor Actuator Phys, 2014, **216**, 295–300.

[35] V. Panwar, K. Cha, J. O. Park and S. Park, Sensor Actuator B Chem, 2012, **161**, 460–470.

[36] V. Panwar, B. S. Kang, J.O. Park and S. Park, Polymer Eng Sci., 2011, **51**, 1730–1741.

[37] M. Luqman, J. W. Lee, K. K. Moon and Y. T. Yoo, J. Ind. Eng. Chem., 2011, **17**, 49–55.

[38] C. C. Chu, Y. W. Wang, L. Wang and T. I. Ho, Synthetic Metals, 2005, **153**, 321-324.

[39] D. G. Dikobe and A. S. Luyt, eXPRESS Polymer Letters, 2009, **3**, 190-199.

[40] T. A. Zawodzinski, V.T. Smith V T, S. Gottesfeld, J. Electrochem. Soc. 1993, **140,** 1041–1047.

[41] M. Rajagopalan, J.H. Jeon, I. K. Oh, Sens. Actuators B 2010, **151**, 198–204.

[41] H. Liana, W. Qian, L. Estevez, H. Liud, Y. Liud, T. Jiangd, K. Wanga, W. Guoe, E. P. Giannelisc, Sensors and Actuators B, 2011, **156,** 187–193.

RSC Advances Accepted Manuscript

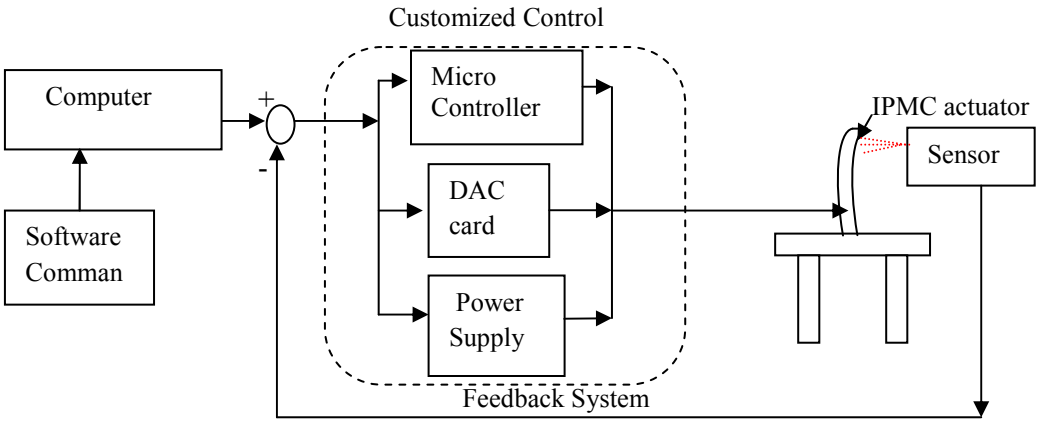

Fig. 1. Schematic diagram for analyzing the bending behaviour of KR-Ag-Pw IPMC actuator

RSC Advances Accepted Manuscript

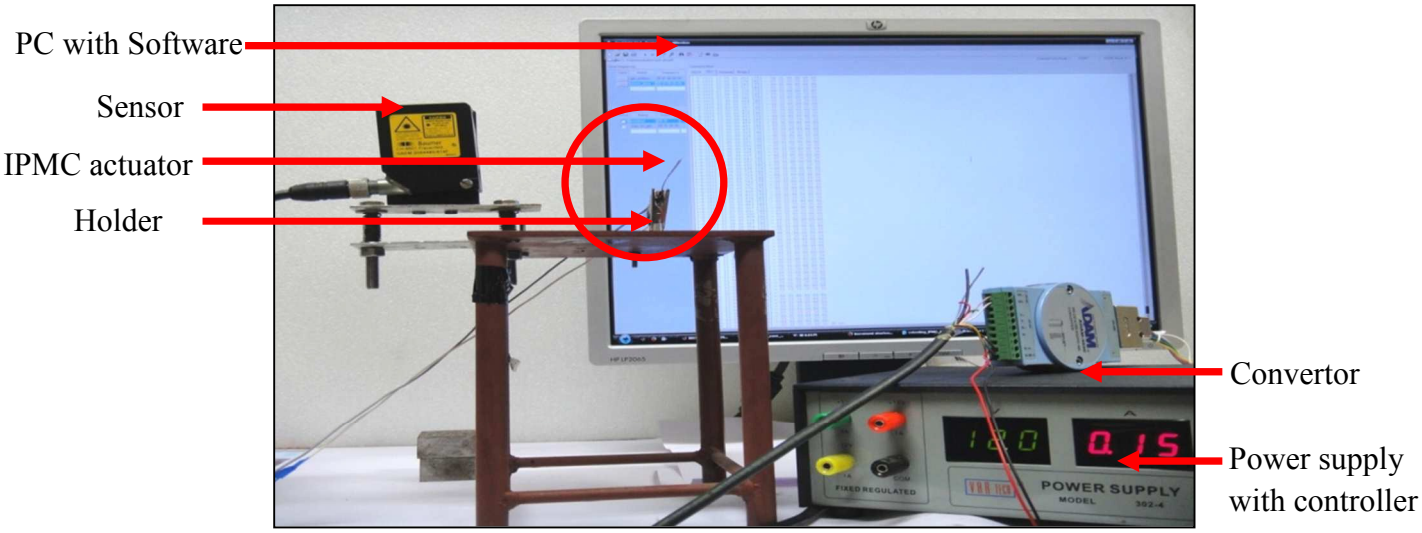

Fig. 2. Actual test setup for bending behaviour of KR-Ag-Pw IPMC actuator.

RSC Advances Accepted Manuscript

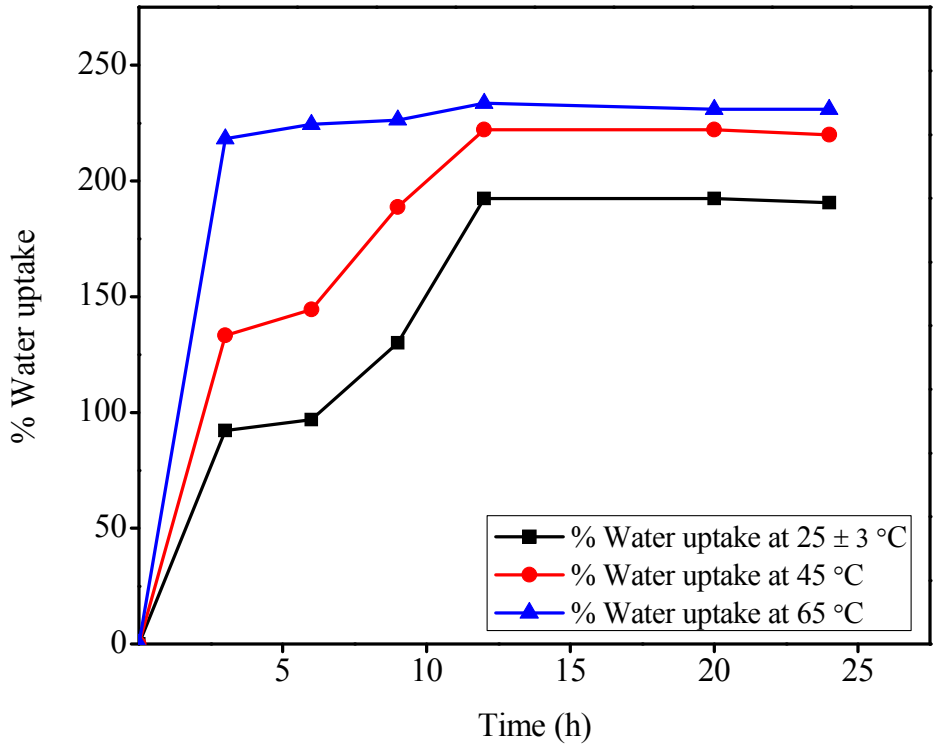

Fig. 3. Water uptake of KR-AgPw ionic polymer actuator membrane at room temperature (25 ± 3 °C), 45 °C and 65 °C for different interval of time.

RSC Advances Accepted Manuscript

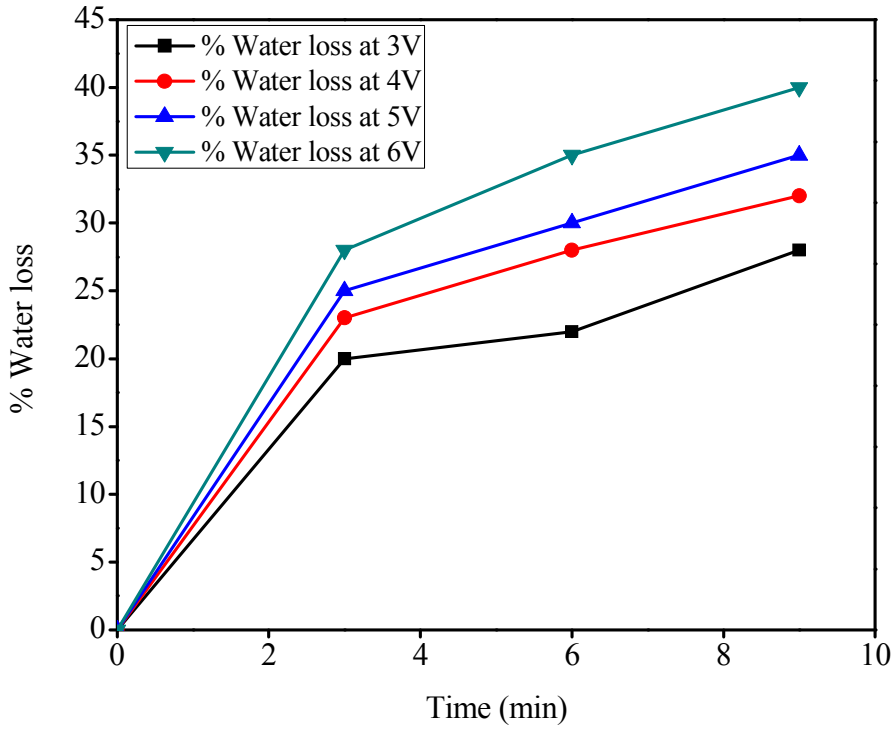

Fig. 4. Water loss of KR-AgPw ionic polymer membrane at 3, 4, 5 and 6 V for 3, 6 and 9 min of time interval.

RSC Advances Accepted Manuscript

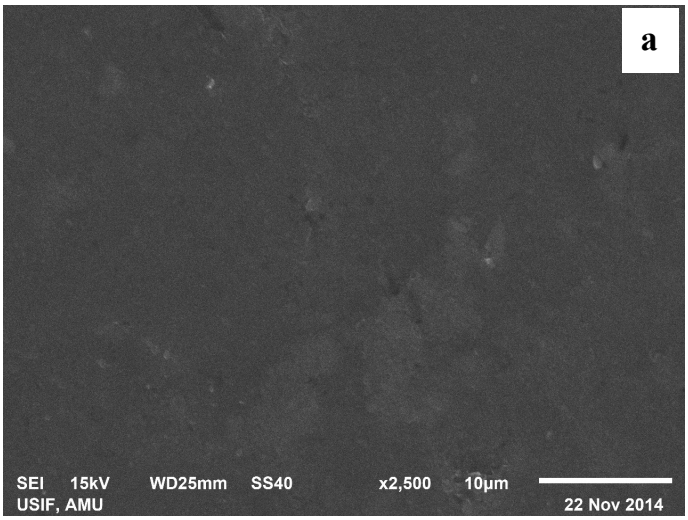

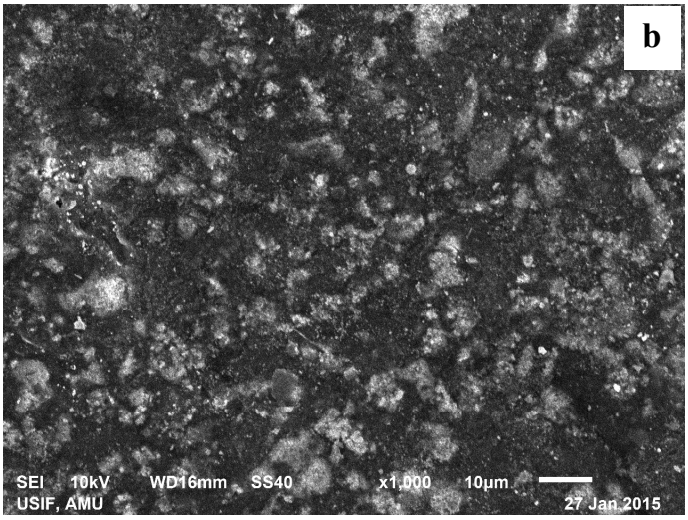

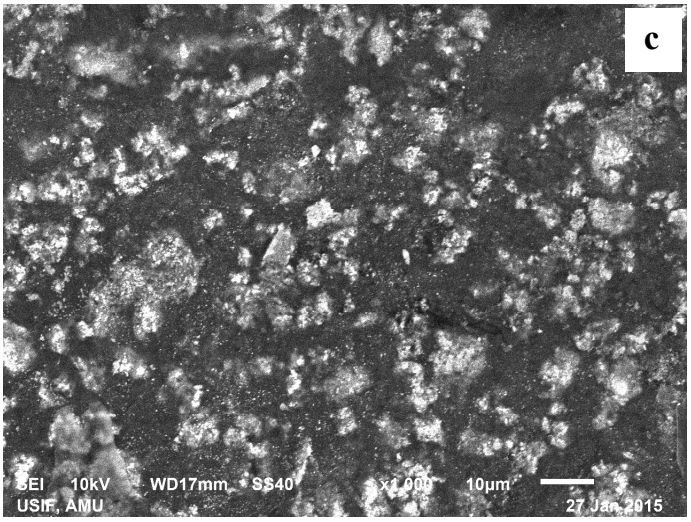

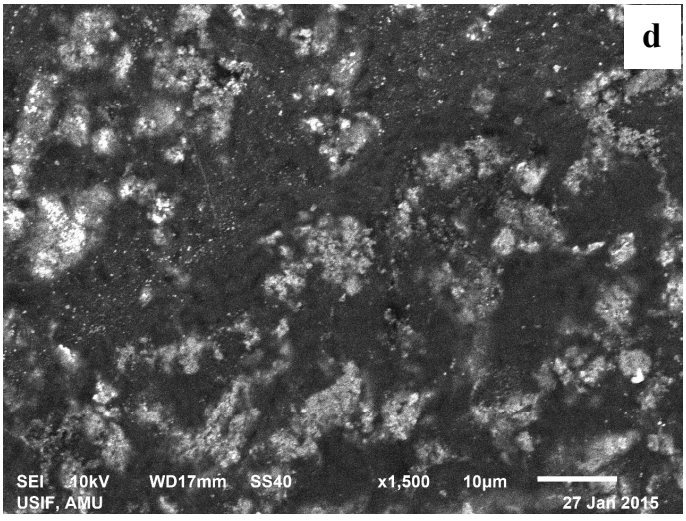

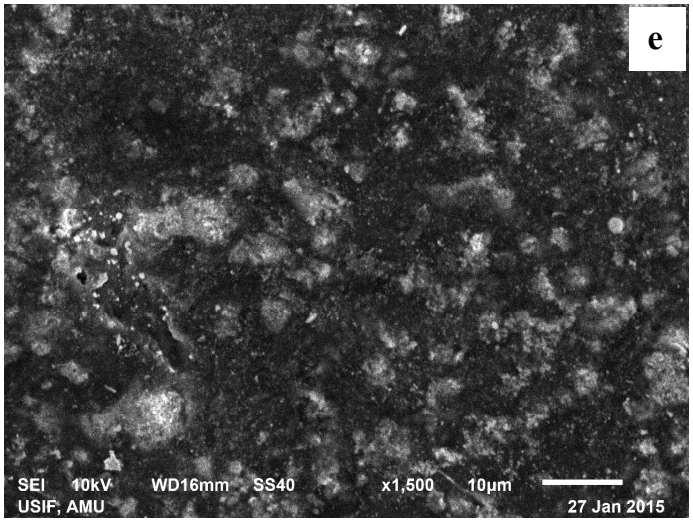

RSC Advances Accepted Manuscript

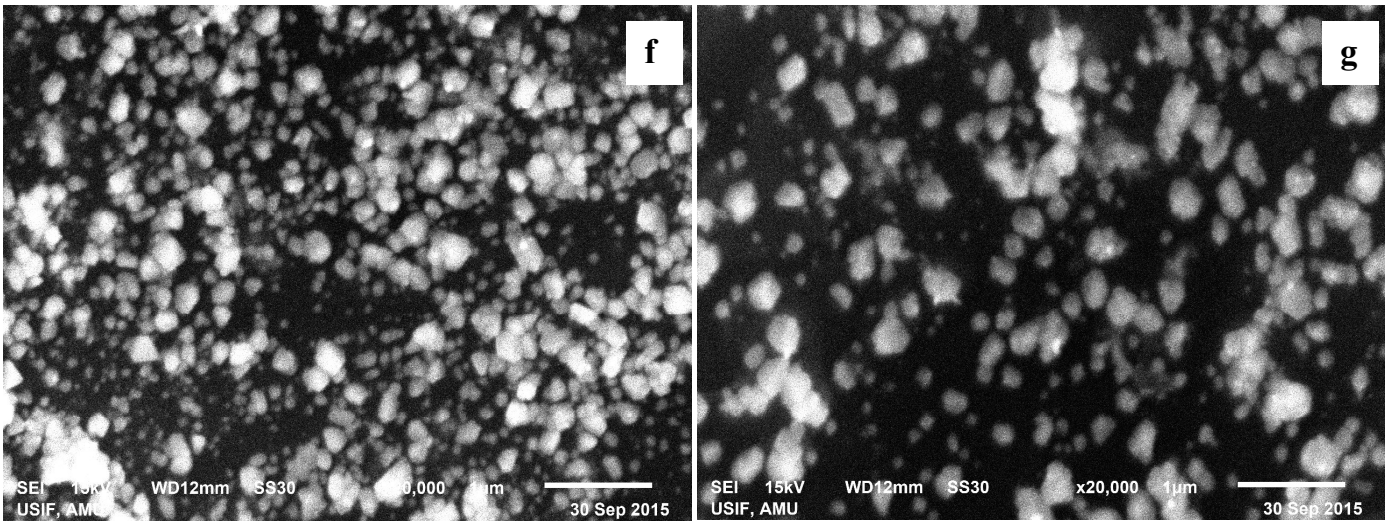

Fig. 5. Scanning electron microscopic images of kraton membrane (a) KR-AgPw ionic polymer membrane (b,d) before and (c,e) after applied electric potential and (f, g) showing silver nanoparticles on the surface of membrane actuator.

RSC Advances Accepted Manuscript

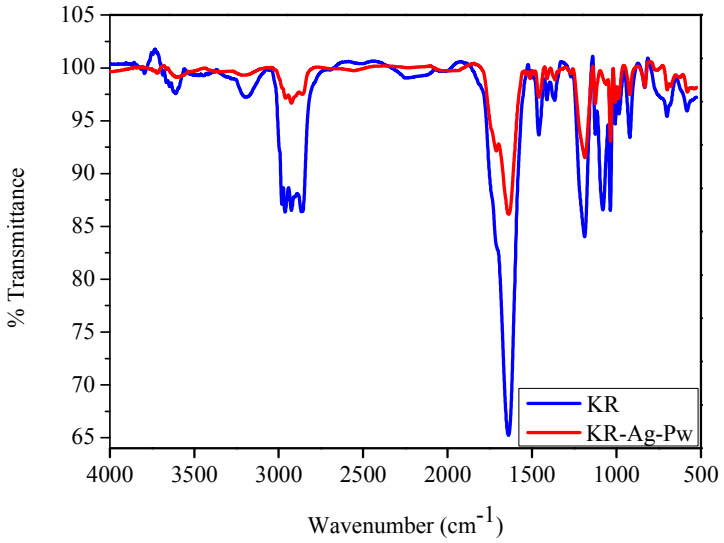

Fig. 6. FTIR spectra of KR and KR-Ag-Pw polymer membranes.

RSC Advances Accepted Manuscript

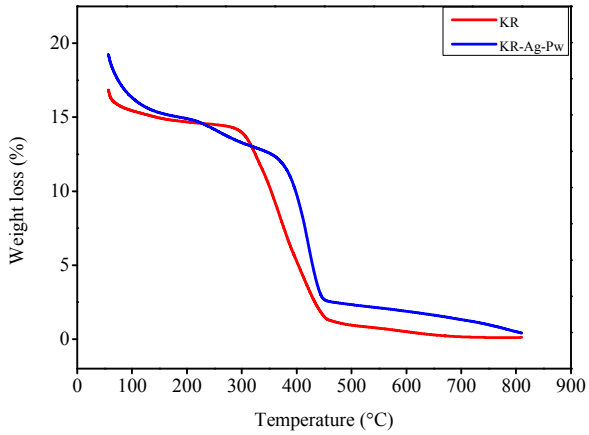

Fig. 7. TGA curves of KR and KR-Ag-Pw polymer membranes.

RSC Advances Accepted Manuscript

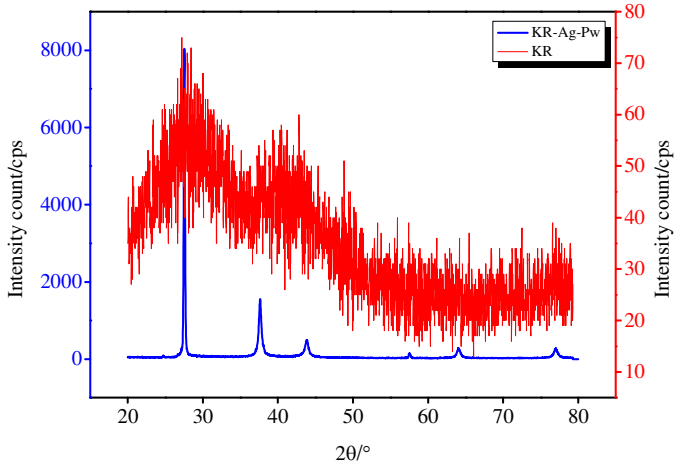

Fig. 8. X-ray diffraction pattern of KR and KR-Ag-Pw polymer membrane.

RSC Advances Accepted Manuscript

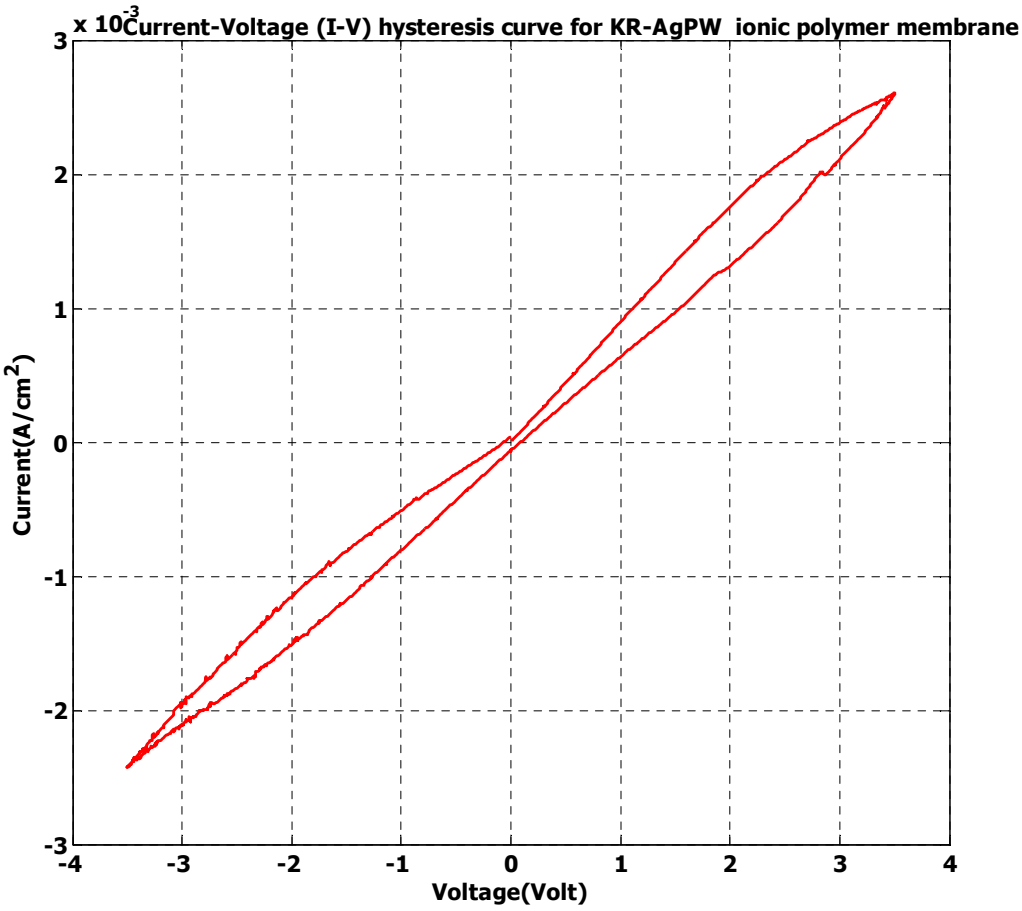

Fig. 9. Cyclic voltammetric curve of KR-AgPw ionic polymer membrane actuator at triangle voltage input of 3.5 V with a step of 50 mV/s.

RSC Advances Accepted Manuscript

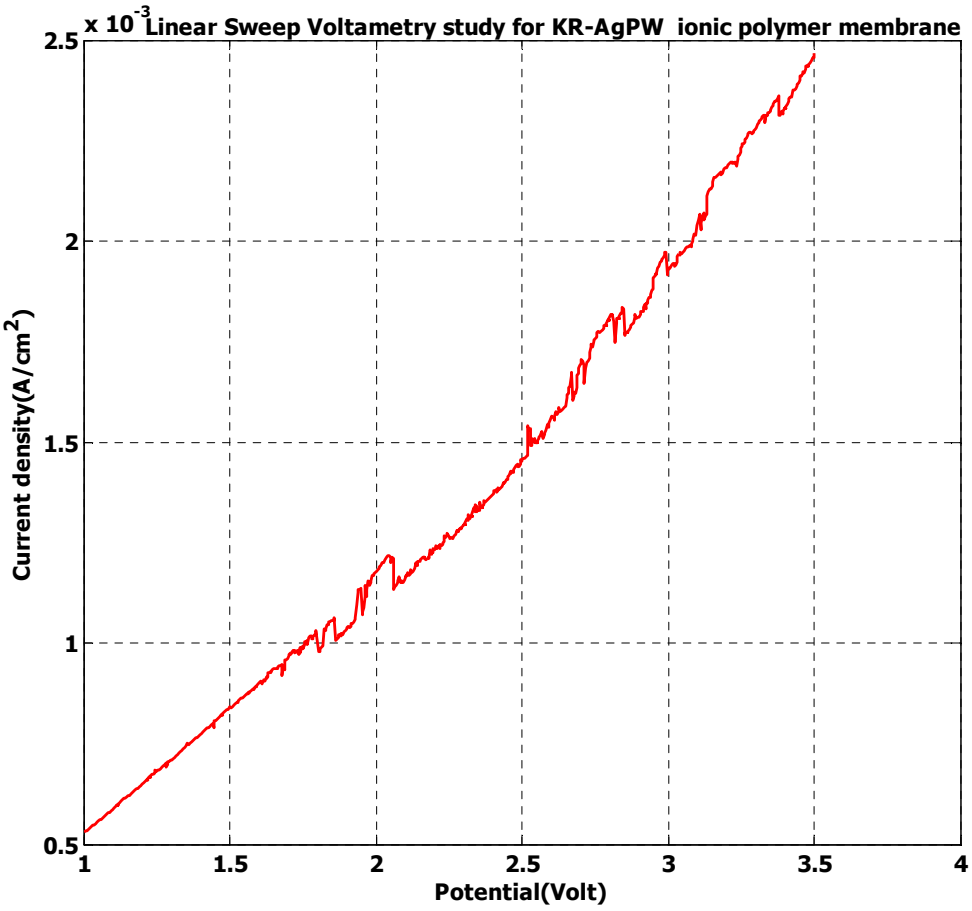

Fig. 10. Linear sweep voltammetric curve of KR-Ag-Pw ionic polymer actuator membrane at 3.5 V with a step of 50 mV/s.

RSC Advances Accepted Manuscript

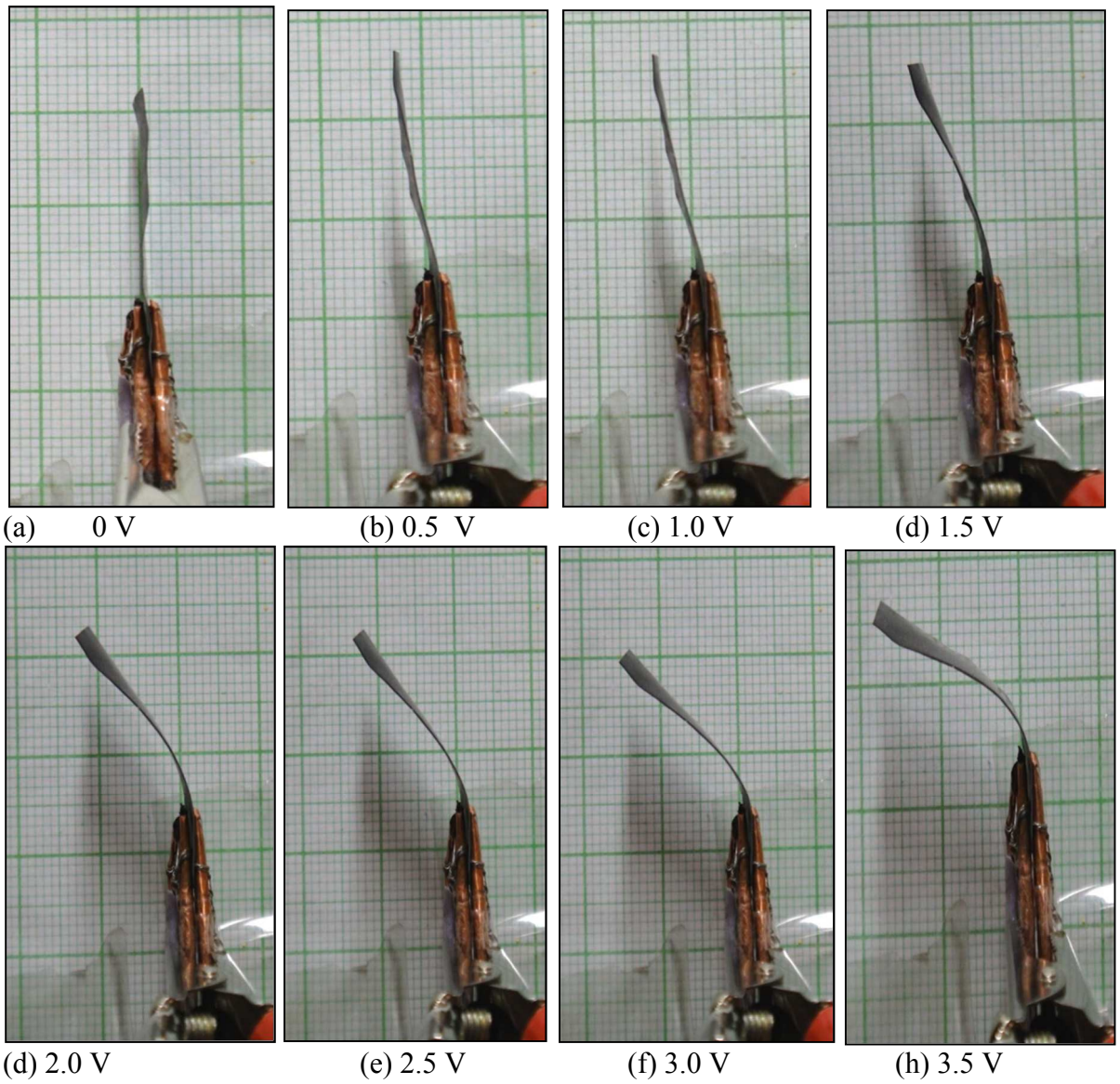

Fig. 11. Bending behaviour of KR-Ag-Pw IPMC actuator.

RSC Advances Accepted Manuscript

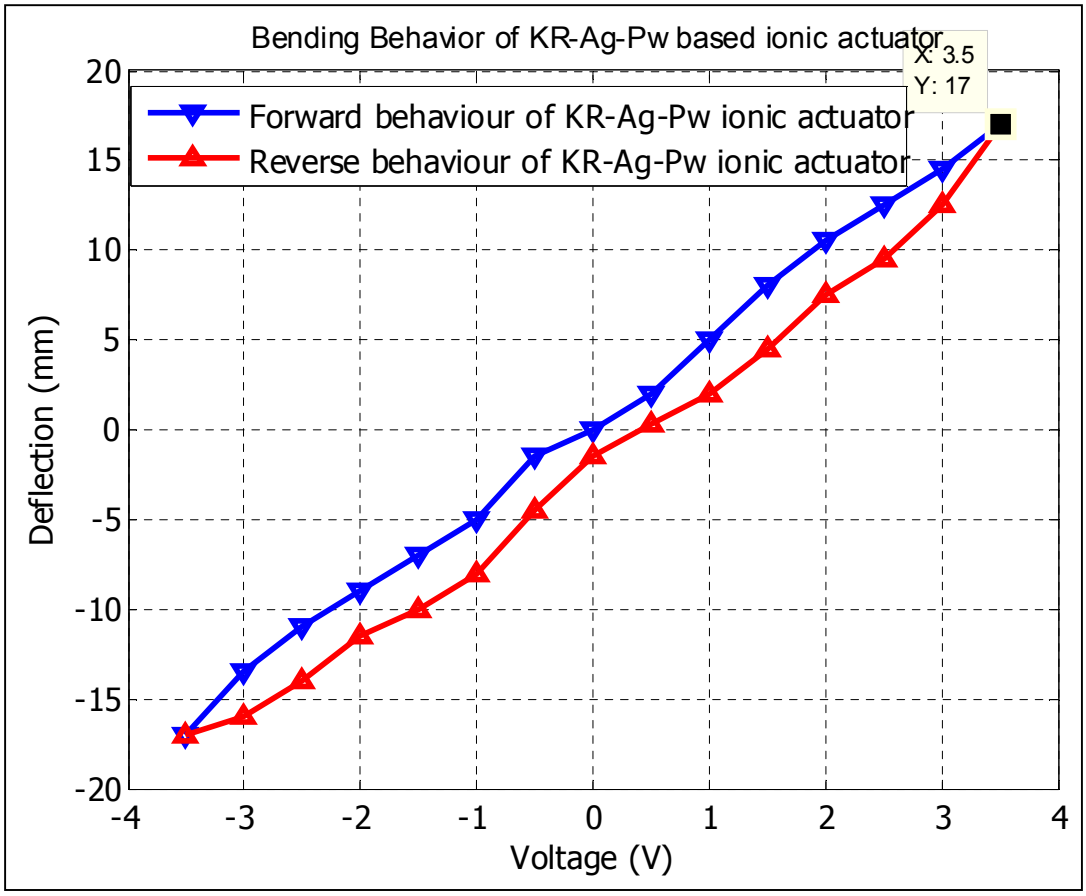

Fig. 12. Bending behavior of KR-Ag-Pw based ionic actuator

RSC Advances Accepted Manuscript

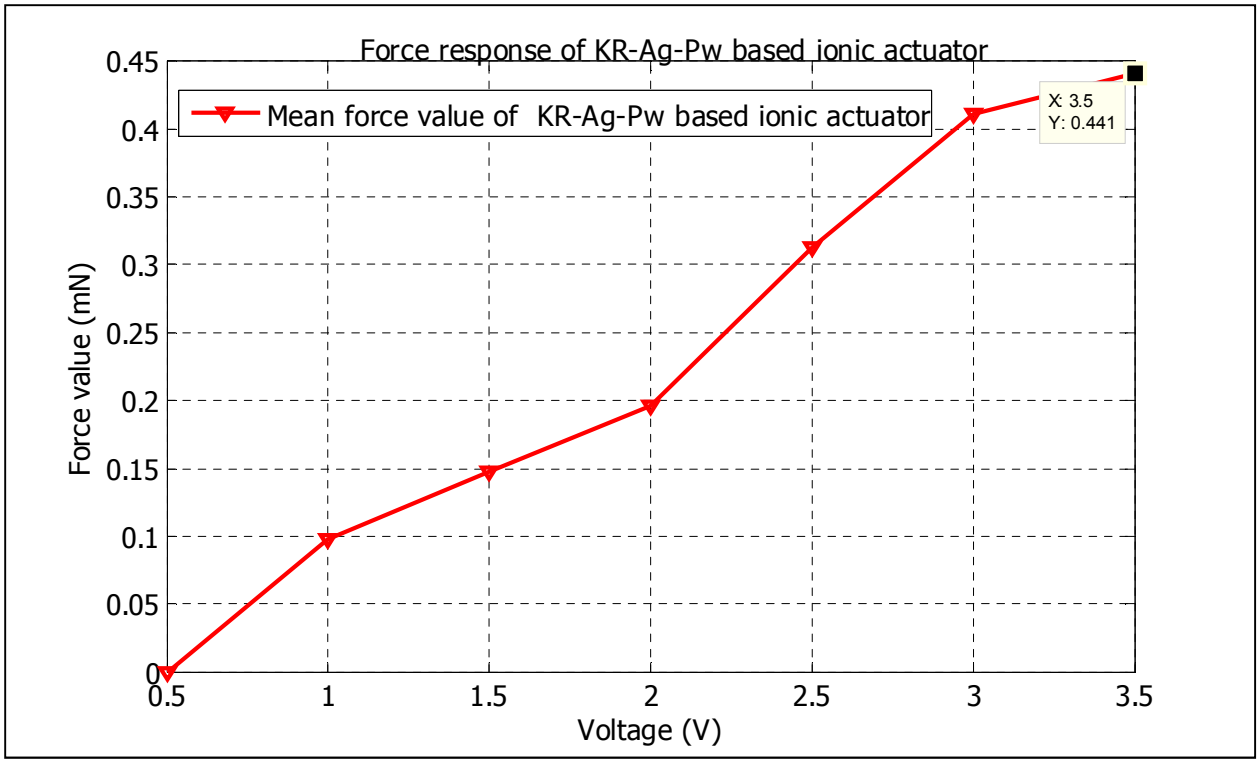

Fig. 13. Mean force value of KR-Ag-Pw based ionic polymer

RSC Advances Accepted Manuscript

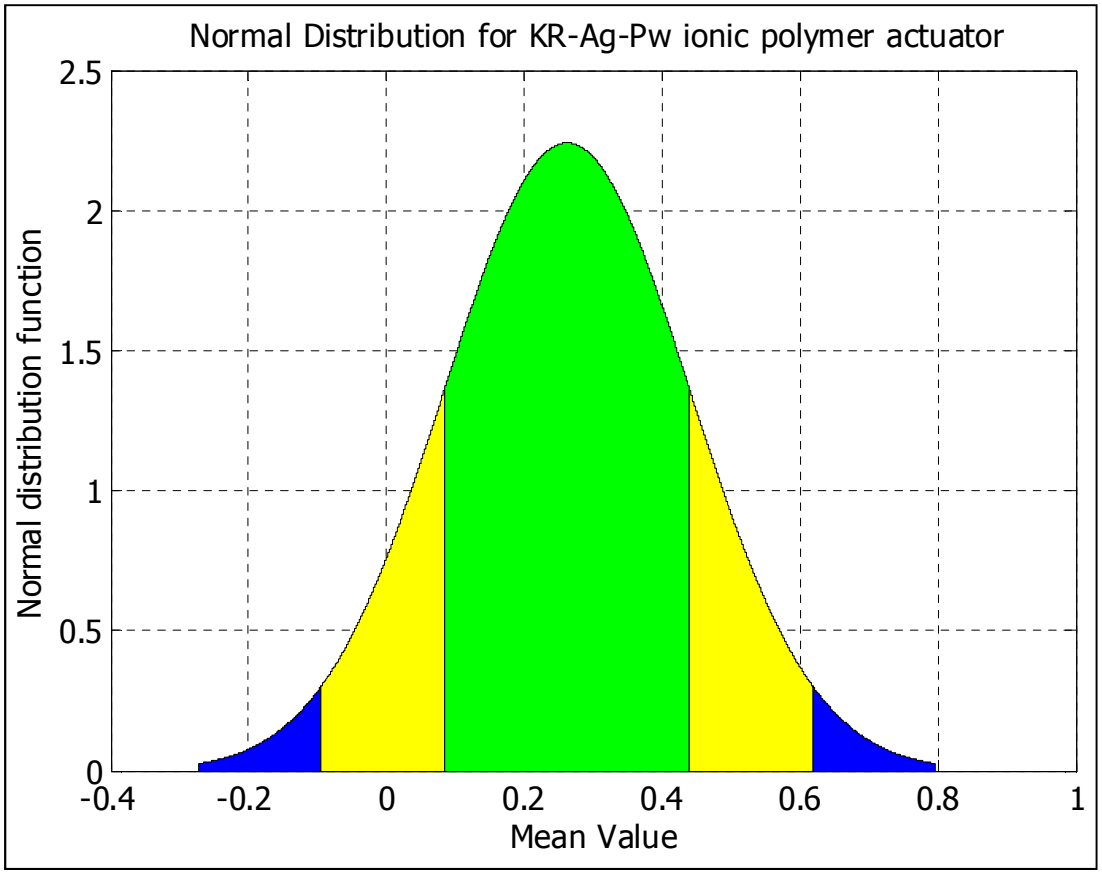

Fig. 14. Normal distribution function for KR-Ag-Pw based ionic actuator

RSC Advances Accepted Manuscript

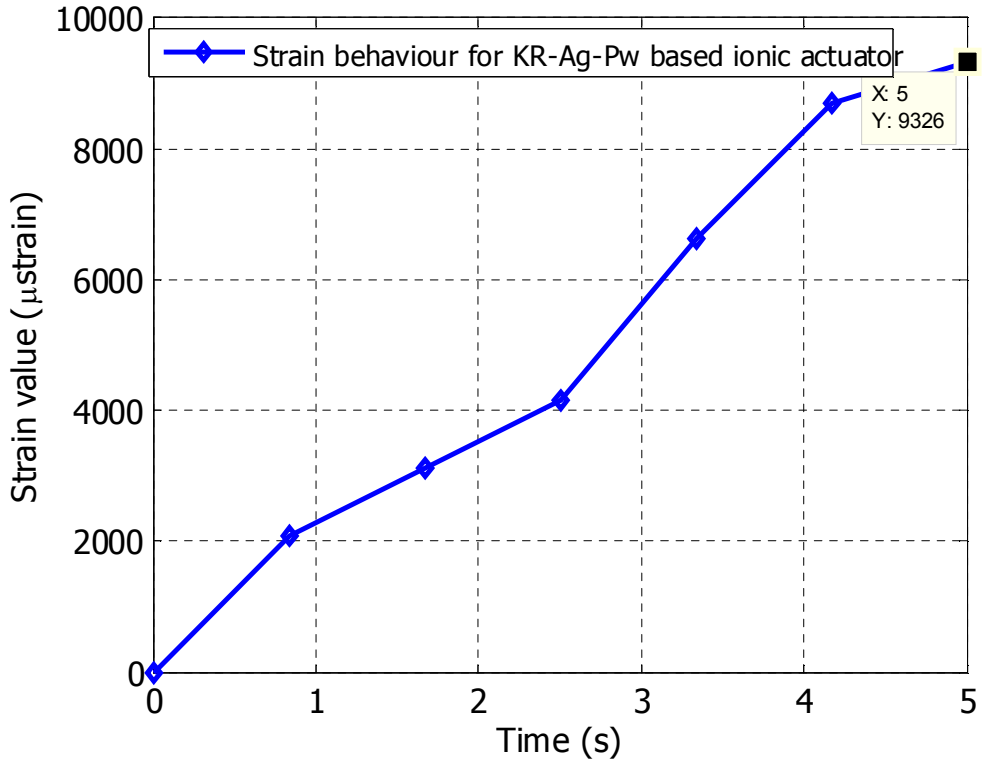

Fig. 15. Strain behavior of KR-Ag-Pw ionic polymer.

RSC Advances Accepted Manuscript

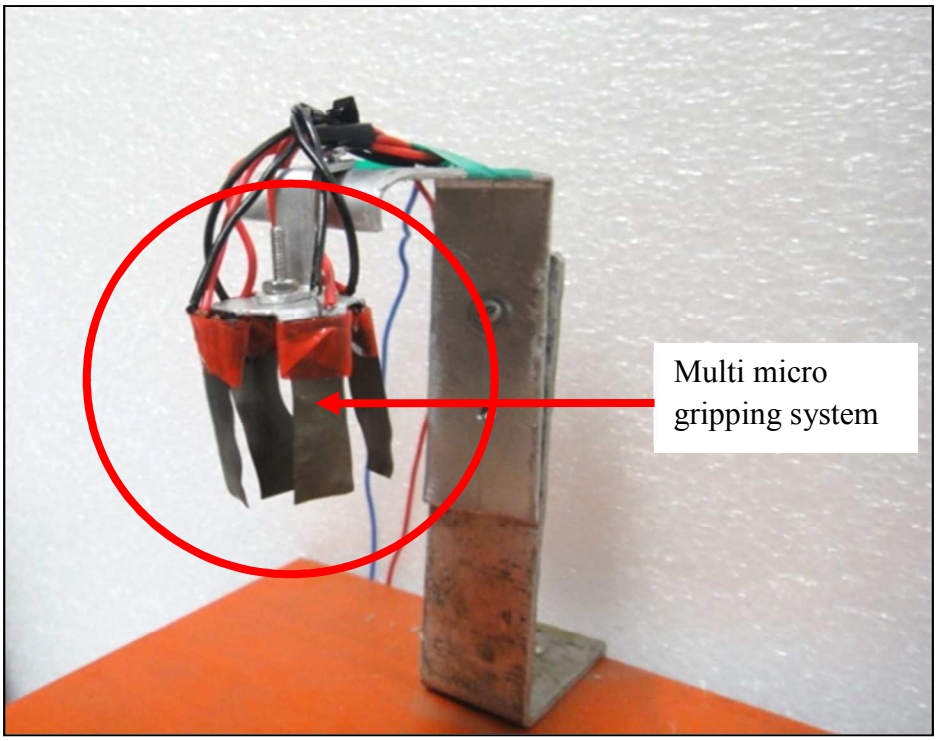

(a) Micro gripping system without holding a object

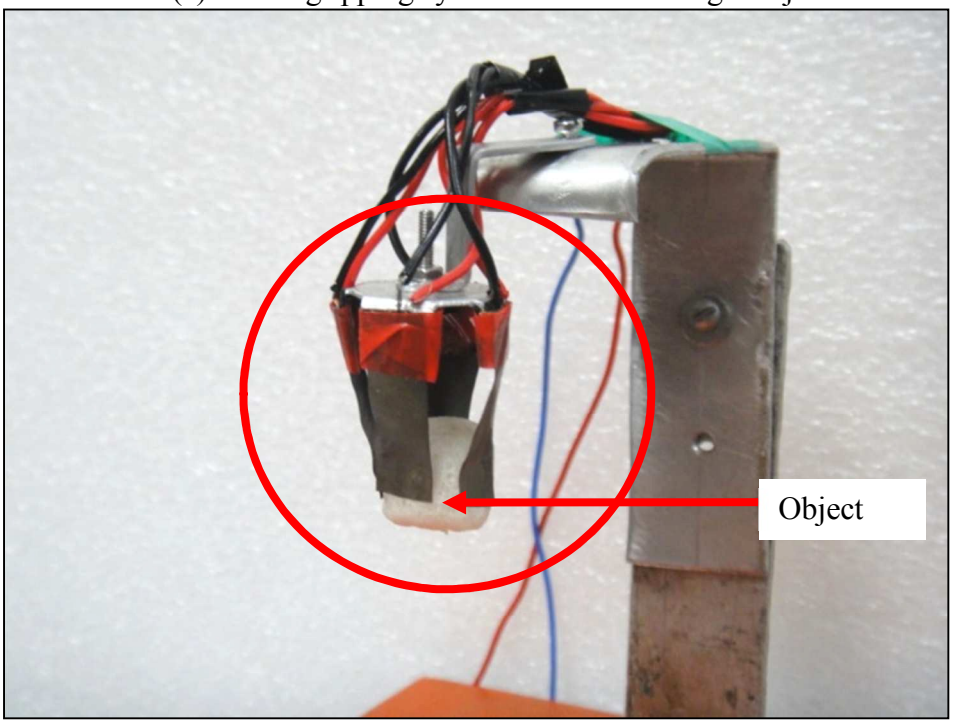

(a) Micro gripping system with holding a object

Fig. 16. Multi fingers based micro gripping system using KR-Ag-Pw based ionic actuator.

RSC Advances Accepted Manuscript

Table 1 Deflection data of KR-Ag-Pw IPMC actuator with voltages.

Voltage *(V)*	Deflection data (mm)					Average value of deflection *D* (mm)
	Deflection *(D1)*	Deflection *(D2)*	Deflection *(D3)*	Deflection *(D4)*	Deflection *(D5)*	
0	0	0	0	0	0	0
0.5	2.1	1.8	1.9	2.2	2.0	2.0
1.0	4.2	4.0	3.9	3.8	4.1	4.0
1.5	5.5	5.6	5.3	5.5	5.6	5.5
2.0	11.1	11.2	10.9	11.0	10.8	11.0
2.5	12.4	12.5	12.2	12.6	12.8	12.5
3.0	14.1	13.9	14.2	13.8	14.0	14.0
3.5	17.0	16.8	16.9	17.1	17.2	17.0

RSC Advances Accepted Manuscript

Table 2. Force data of KR-Ag-Pw based ionic actuator

S. No.	Voltage (V)	Force value (F1) in mN	Force value (F2) in mN	Force value (F3) in mN	Force value (F4) in mN	Force value (F5) in mN	Average Force value (F) in mN
1.	0.5	0	0	0	0	0	0
2.	1.0	0.088	0.117	0.107	0.078	0.098	0.098
3.	1.5	0.166	0.156	0.156	0.137	0.117	0.147
4.	2.0	0.186	0.215	0.176	0.166	0.235	0.196
5.	2.5	0.294	0.313	0.333	0.304	0.323	0.313
6.	3.0	0.431	0.411	0.392	0.421	0.402	0.411
7.	3.5	0.441	0.460	0.421	0.431	0.451	0.441
	Mean						0.2620
	Standard Deviation (SD)						0.1781
	Normal Deviation (ND)						0.7590
	Repeatability						99.2410

RSC Advances Accepted Manuscript

Table 3. Comparison of SPVA-Py-Pt based IPMC with other IPMC actuators

Properties	KR-Ag-Pw based IPMC	Nafion Based IPMC [40]	Kraton Based IPMC actuator [34]	Sulfonated polyetherimide [33]	Carbon Nano tube Actuator [41]
Water uptake	82.3%	16.70%	309.69%	26.4%	25.1 %
Tip displacement	17.0 mm	12 mm	40 mm	2.7 mm	20 mm
Ion-exchange capacity	2 meq g^{-1}	0.98 meq g^{-1}	1.9 meq g^{-1}	0.553 meq g^{-1}	0.71 meq g^{-1}
Proton conductivity	1.87×10^{-3} S/cm	9.0×10^{-3} S/cm	17.15 S/cm	1.4×10^{-3} S/cm	5.7×10^{-3} S/cm
Current density	50 mV/cm^2	0.03 mV/cm^2	0.05 mV/cm^2	5×10^{-4} mV/cm^2	-

RSC Advances Accepted Manuscript